Japan Society of Histochemistry and Cytochemistry
Established 1959

Acta Histochem. Cytochem. 50 (6): 159–168, 2017
doi: 10.1267/ahc.17027

CCN3 Expression Marks a Sulfomucin-nonproducing Unique Subset of Colonic Goblet Cells in Mice

Shintaro Akiyama[1], Wakana Mochizuki[1], Yoichi Nibe[1], Yuka Matsumoto[1], Kei Sakamoto[2], Shigeru Oshima[1], Mamoru Watanabe[1] and Tetsuya Nakamura[3]

[1]Department of Gastroenterology and Hepatology, Graduate School, Tokyo Medical and Dental University, [2]Department of Oral Pathology, Graduate School, Tokyo Medical and Dental University and [3]Department of Advanced Therapeutics for GI Diseases, Graduate School, Tokyo Medical and Dental University, 1–5–45 Yushima, Bunkyo-ku, Tokyo 113–8519, Japan

Received September 6, 2017; accepted October 18, 2017; published online November 23, 2017

Intestinal goblet cells are characterized by their unique morphology and specialized function to secrete mucins. Although it is known that they are a heterogeneous population of cells, there have been few studies that relate the expression of a particular gene with functionally distinct subpopulations of intestinal goblet cells. Here we show that *CCN3*, a gene encoding a member of the CCN family proteins, is induced by inhibition of Notch signaling in colonic epithelial cells and expressed in goblet cells in mice. We demonstrate that *CCN3* expression is confined to a subpopulation of goblet cells in the lower crypt of the proximal and middle colon. In addition, *CCN3*+ cells in the colon correlate well with the cells that are positive for alcian blue (AB) staining but negative for high-iron diamine (HID) staining in histology. We also show that *CCN3*+ cells, which are absent in the normal distal colon, transiently and ectopically emerge in regenerating crypts during the repair phase of DSS-induced colitis model. Our study thus suggests that CCN3 labels a unique subpopulation of sulfomucin-nonproducing colonic goblet cells that function in both normal and diseased colonic epithelia.

Key words: CCN3/Nov, goblet cells, sulfomucin, *in situ* hybridization, DSS-induced colitis

I. Introduction

Intestinal goblet cells are characterized by their unique morphology and specialized function to secrete mucus components mainly composed of Muc2 [2, 36]. Goblet cells and other two secretory lineages, enteroendocrine and Paneth cells, arise from a common progenitor that originates from *Lgr5*+ stem cells residing at the crypt base. Several lines of evidence show that inhibition of the Notch signaling pathway, a conserved intercellular signaling system critical for many biological processes, drives differentiation of crypt cells towards secretory lineages [25, 35].

Studies have proposed that intestinal goblet cells contain functionally distinct subpopulations. For example, acidic mucin-producing goblet cells, which are broadly detected by alcian blue (AB) staining, do not completely coincide with those produce sulfomucin, a form of acidic mucin detectable by high-iron diamine (HID) staining [32, 33]. This suggests that AB-positive (AB+) goblet cells contain two distinct subpopulations: cells that produce a large amount of sulfomucin and are HID-positive (HID+), and those produce less or no sulfomucin and are HID-negative (HID−). However, there have been few reports that relate the expression of a particular gene with such subpopulations of goblet cells that produce mucins with different chemical modifications. Thus, we were interested in identifying genes that are specifically expressed in goblet cells

Correspondence to: Tetsuya Nakamura MD, PhD, Department of Advanced Therapeutics for GI Diseases, Graduate School, Tokyo Medical and Dental University, 1–5–45 Yushima, Bunkyo-ku, Tokyo 113–8519, Japan. E-mail: nakamura.gast@tmd.ac.jp

by screening the Notch-repressed genes in the colon, which may include not only those regulating differentiation toward secretory cells but also those functioning in subpopulations of secretory cell types. Previous studies demonstrated that γ-secretase inhibitors (GSIs), which act as inhibitors for the Notch signaling, are useful to identify or investigate the genes expressed in secretory cell types in the intestine [24, 31]. Hence, this chemical inhibition approach was applied in our study to inhibit Notch signaling in mouse colonic cells, which are isolated from normal, non-tumorous tissues and three dimensionally cultured as a pure epithelial population called an organoid.

Members of the CCN family are a matricellular protein, which is secreted and assembled with extracellular matrix to act on target cells [13, 16]. CCN3 (also known as Nov), one of the founding members of this family, is known to be involved in various biological processes, such as angiogenesis [17] and maintenance of stem cells [9]. CCN3 is also implicated in many pathobiological processes such as inflammation [19] and wound healing [18]. Despite such multiple functions of CCN3 in normal and diseased tissues, there has been no report of expression and/or function of CCN3 in the intestine. By microarray analysis of gene expression in mouse colonic organoids, we here show that *CCN3* is a gene induced by inhibition of Notch signaling in mouse colonic epithelial cells. We also show that expression of *CCN3* is confined to a unique subpopulation of goblet cells, which are characterized as being AB+ and HID− and present only in the proximal and middle colon under physiological condition. In addition, we demonstrate that the expression pattern of *CCN3* changes significantly during the epithelial regeneration phase in an experimental colitis model in mice.

II. Materials and Methods

Mice

C57BL6 mice were maintained in the animal facility of Tokyo Medical and Dental University (TMDU). Male mice at 8 weeks of age were used in this study. Tissue samples were removed from mice immediately after they were sacrificed by cervical dislocation. All animal experiments were performed with the approval of the Institutional Animal Care and Use Committee of TMDU.

Organoid culture

Crypts were separately isolated from proximal and distal halves of the colon as described previously [39]. Briefly, crypts were isolated by digesting the tissue with 500 U/ml collagenase XI (Sigma), 0.4 U/ml dispase (Roche), and 1 mM dithiothreitol. Obtained crypts were suspended in the collagen type I solution (Nitta Gelatin Inc.) and placed in 24-well plates. After polymerization, 500 μl of Advanced DMEM/F12 containing 1% BSA (Sigma), 30 ng/ml mWnt3a, 500 ng/ml mRspo1, 50 ng/ml mHGF, 50 ng/ml mNoggin (all from R&D Systems), and 20 ng/ml mEGF (Peprotech) were added to each well. When indicated, organoids were treated with either 1 μM LY411575 (Santa Cruz Biotechnology), a GSI, or vehicle (DMSO) alone for 48 hours from day 3 to day 5 of culture.

Gene expression analyses

Total RNA extraction was carried out using the RNeasy Mini Kit (Qiagen). For microarray analysis, RNA samples from distal colon organoids before (n = 1) and after (n = 1) treatment with LY411575 (1 μM) were outsourced to Kamakura Techno-Science Inc. Synthesis, amplification and Cy5-labeling of probes and their hybridization on 3D-Gene Mouse Oligo chip 24k (Toray Industries) were performed according to the supplier's protocol (www.3d-gene.com). Data were acquired on 3D-gene Scanner (Toray Industries Inc.) and normalized by using global normalization method (the median of the detected signal intensity was adjusted to 25). Genes that showed >2.5-fold differences in expression values between two samples are presented (Supplementary Tables S1, S2). For semi-quantitative RT-PCR, RNA samples from organoids before (n = 3) and after 48-hr treatment with either 1 μM LY411575 (n = 3) or vehicle (DMSO) alone (n = 3) were isolated. Aliquots of 300 ng of total RNA were used for cDNA synthesis in 21 μl of reaction volume. One microliter of cDNA was used for the following RT-PCR. Primer sequences and the detail of reactions are listed in Supplementary Table S3. PCR products were separated on agarose gels and visualized using ImageLab (Bio-Rad).

Induction of colitis

Acute colitis was induced by giving 8-week-old male mice drinking water containing 3.0% dextran sulfate sodium (DSS) (MW 36,000–50,000: MP Biomedicals) for 5 days. Control mice received drinking water without DSS. All mice were weighed every day. On day 5, 10 and 16 of DSS administration, mice were sacrificed for tissue analysis (n = 3 for each group per time point).

Histology

Intestines were fixed in 4% paraformaldehyde, dehydrated in 20% sucrose in PBS, embedded in OCT compound (Tissue Tek), and sectioned at 10 μm thickness. AB staining (pH 2.5) and HID staining were performed as described previously [33]. When indicated, sections were doubly stained for AB and HID. Images were acquired on a microscope BZ-X710 (KEYENCE). Quantification of AB+ or HID+ cells per crypt was made by randomly choosing well-oriented, full-length crypts on sections of the cecum or nine segments (segment 1–9) along the proximal-to-distal axis of the colon. By examining 5 crypts in each section originating from individual mice (n = 3), 15 crypts were assessed in total for AB+ and HID+ cells in each intestinal segment.

In situ hybridization (ISH)

A digoxigenin (DIG)-labeled RNA probe that corresponds to a part of mouse *CCN3* mRNA (nucleotides 323–847; GenBank NM010930.4), and a fluorescein isothiocyanate (FITC)-labeled RNA probe for mouse *Muc2* mRNA (nucleotides 25–443; GenBank NM023566.3) were generated by *in vitro* transcription system (Roche). Frozen sections of intestinal tissues were rehydrated, treated with HCl, digested in proteinase K, postfixed, treated in acetic anhydride solution, and hybridized overnight at 60°C as described previously [8]. For single detection of *CCN3*, sections were incubated with an alkaline phosphatase (AP)-conjugated anti-DIG antibody (Roche) and then reacted with nitroblue tetrazolium/5-bromo-4-chloro-3-indolyl phosphate solution for color development. Quantification of *CCN3*+ cells was performed as described for counting AB+/HID+ cells (total 15 crypts for each segment). Double ISH was performed as previously described [37]. Tissues were hybridized with the probes for *Muc2* and *CCN3* simultaneously at 60°C. For detection of the FITC probe, the sections were incubated with a horseradish peroxidase (HRP)-conjugated anti-FITC antibody (Jackson ImmunoResearch). The sections were then treated with TSA-Plus (DNP) system (Perkin Elmer). Then the DNP signals on the sections were detected by anti-DNP antibody conjugated to an Alexa Fluor 488 (Molecular Probe). At this point, an AP-conjugated anti-DIG antibody (Roche) was included in the incubation for the detection of the DIG probes. Sections were reacted with HNPP fluorescent detection set (Roche) to visualize AP conjugates. Nuclei were counterstained with Hoechst33342. Images were acquired on a microscope BZ-X710 (KEYENCE) and processed using Adobe Photoshop software when necessary.

Western blot

Total protein was extracted from the aorta or each segment of the intestine by tissue homogenization in a RIPA buffer (1% deoxycholic acid, 0.1% SDS, 1% NP40) containing protease/phosphatase inhibitor cocktail (Pierce). Protein concentrations were determined by BCA protein assay kit (Pierce). Twenty micrograms of aorta extract or 10 μg of intestinal extracts were resolved on NuPage precast 4%–12% Bis-Tris gels (Invitrogen) and transferred to polyvinylidene difluoride membranes (Millipore). The membranes were blocked in 5% skim milk solution, incubated with an anti-CCN3 antibody [14], and then reacted with an HRP-conjugated mouse anti-rabbit secondary antibody (Jackson). The proteins were visualized using Luminata Forte Western HRP substrate (Millipore). Membranes were reprobed with an anti-β actin primary antibody (Sigma Aldrich Corp.) and an HRP-conjugated goat anti-mouse secondary antibody (Jackson) to show the loading control. Images were acquired using ImageLab (Bio-Rad) and processed using Adobe Photoshop software.

III. Results

CCN3 is induced by inhibition of Notch signaling in colonic epithelial cells

On the assumption that the genes induced by Notch signal inhibition may include those functioning in subpopulations of secretory lineages such as goblet cells, we cultured epithelia of the mouse distal colon as organoids and treated them with 1 μM LY411575, a GSI for 48 hours to perform gene expression analyses. mRNAs were extracted from organoids before and after GSI treatment and assessed by microarray analysis. This identified 143 genes that were up-regulated in GSI-treated organoids as compared to the pretreatment control by more than 2.5-fold (Supplementary Table S1). They included genes encoding transcription factors known to function in secretory lineages such as *Atoh1* [38] and *Neurog3* [10]. Genes expressed preferentially in enteroendocrine cells (*ChgA, ChgB* [28]), goblet cells (*Guca2a* [3], *Clca3* [15]) and a *cKit*-expressing subset of goblet cells (*Reg4, Spink4, Spdef, Agr2, Tff3* [29]) were also up-regulated in GSI-treated organoids. Although normal mouse colon epithelium lacks Paneth cells, several Paneth cell-specific genes, such as *Lysozyme* and *Ang4*, were shown to be up-regulated. We considered this reasonable as previous studies showed that *Lysozyme* [5] and *Ang4* [6] are expressed in the colon epithelium under certain circumstances. We next validated our microarray data by semi-quantitative RT-PCR. mRNA expression levels of all genes mentioned above (*Atoh1, Neurog3, ChgA, B, Guca2a, Clca3, Reg4, Spink4, Spdef, Agr2, Tff3, Lysozyme and Ang4*) were significantly increased in GSI-treated organoids compared with pretreatment controls (Fig. 1). We previously showed that the proportions of different cell types, such as *Lgr5*+ stem cells and goblet cells, change over time in organoids even during the conventional culture [39]. This means that the different levels of gene expression between GSI-treated organoids and pretreatment controls can result from such temporal change in cell composition. As expected, when the organoids were cultured for 48 hours in the presence of vehicle (DMSO) alone and analyzed, mRNA expression levels of many genes were significantly altered as compared to pretreatment controls (Fig. 1). However, we found that the expression levels of *Atoh1, Neurog3, ChgA, B, Guca2a, Clca3, Reg4, Spink4, Spdef, Agr2, Tff3, Lysozyme and Ang4* were significantly higher than those in organoids treated with vehicle alone, which confirmed that they were up-regulated as a result of Notch signal inhibition (Fig. 1). It remains unclear whether the different expression of genes between pretreatment controls and DMSO-treated organoids is due to the cell composition change during culture or it is also caused by the action of DMSO; however, we did not pursue this further in this study.

The microarray data also identified 45 genes that were down-regulated by more than 2.5-fold (Supplementary Table S2). Unexpectedly, a transcriptional factor *Hes1*, a

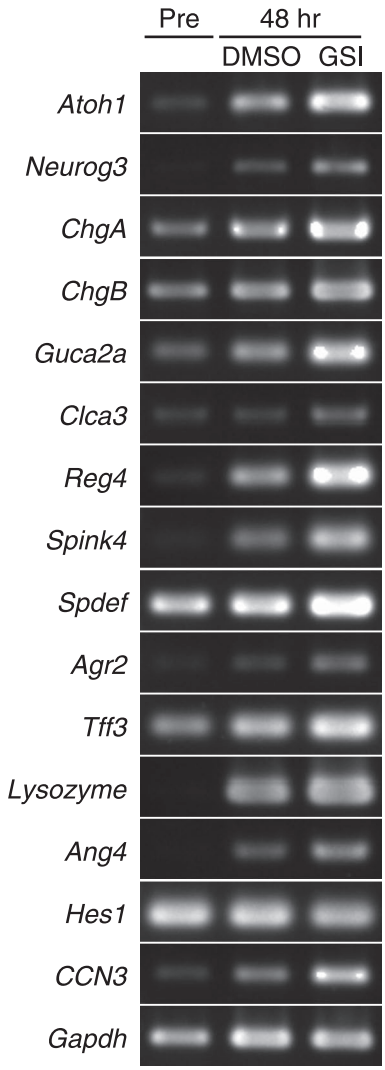

Fig. 1. *CCN3* expression is up-regulated in GSI-treated colon organoids. Crypts isolated from the distal half of the colon were cultured as organoids. They were treated with either 1 μM LY411575, a γ-secretase inhibitor (GSI) or vehicle (DMSO) alone for 48 hours from day 3 to day 5 of culture. Total RNA was extracted from organoids on day 3 as a pretreatment control (Pre) or from those cultured in the absence (DMSO) or presence of GSI on day 5. Semi-quantitative RT-PCR was performed for the indicated genes. Representative data of three independent experiments are shown.

well-known target gene of the Notch signaling [11, 35], showed 1.1-fold reduction and was not included in the list of highly down-regulated genes. RT-PCR supported this data as *Hes1* mRNA was not significantly repressed by GSI (Fig. 1). However, our data are consistent with a previous study where *Hes1* mRNA was shown to stay unaltered even after Notch inhibition for 4 days in rat duodenal cells [22]. We thus assumed that inability of our analysis to detect *Hes1* repression was not due to insufficient action of GSI but rather to other mechanisms such as long stability of pre-existing *Hes1* mRNA. Collectively, it was suggested that our microarray data would be useful to identify genes induced by Notch signal inhibition in colonic epithelial cells, although they might not be sensitive enough to detect some down-regulated genes.

We were interested in analyzing *CCN3*, a gene encoding a member of matricellular CCN family proteins, which appeared on the list of genes induced by GSI (Supplementary Table S1). A previous study showed that CCN3 directly associates with the extracellular domain of Notch1 and activates its downstream signaling to suppress differentiation of myogenic cells [30]. However, there have been no reports that analyzed the expression or function of CCN3 in the colon. By RT-PCR, we found that *CCN3* mRNA was markedly up-regulated in GSI-treated organoids compared with pretreatment controls or untreated organoids (Fig. 1). A similar result was obtained in organoids derived from the proximal colon (not shown), suggesting that expression of *CCN3* is negatively regulated by Notch signaling throughout the length of mouse colon.

Expression of CCN3 is confined to AB+/HID− goblet cells localized in lower crypts of the proximal and middle colon

To analyze the distribution pattern of *CCN3* expression in the intestine, we performed ISH. Interestingly, we found that *CCN3* was differently expressed in the epithelium along the proximal-to-distal axis of the intestine. Expression of *CCN3* was not detectable in the small intestine and cecum (Fig. 2A). In the colon, its expression was clearly observed in the proximal and middle segments, but declined to undetectable levels in the distal colon (Fig. 2A). In the proximal and middle colon, *CCN3* expression was confined within lower half or two thirds of crypts and undetectable in the surface epithelium (Fig. 2A). We did not observe obvious staining for *CCN3* mRNA in non-epithelial tissue components, such as smooth muscle cells, in any intestinal segments. The unique distribution pattern of *CCN3* along the proximal-to-distal axis was confirmed by semi-quantitative RT-PCR. *CCN3* mRNA was detected in the epithelial tissue obtained from the proximal and middle colon, but was absent in the small intestine or in the distal colon (Fig. 2B).

We next attempted to detect CCN3 protein expression by immunohistochemistry. However, our attempts were unsuccessful since the anti-CCN3 antibody yielded high background signals in the mouse intestine. Thus, to confirm the CCN3 expression at the protein level, we performed western blot analysis. The antibody reacted with a protein of around 50 kDa in the extract of aorta that we used as a positive control [40] (Fig. 2C). Under this condition, a distinct band of slightly lower molecular weight than that seen in aorta samples, was detected in the proximal and middle colon but not in the distal colon or small intestine (Fig. 2C). Previous reports described that the molecular size of CCN3 protein varies depending on its modifications in different tissues [4, 34]. Thus, we concluded that the band detected only in the proximal and middle colon represented the expression of CCN3 protein in those colonic segments.

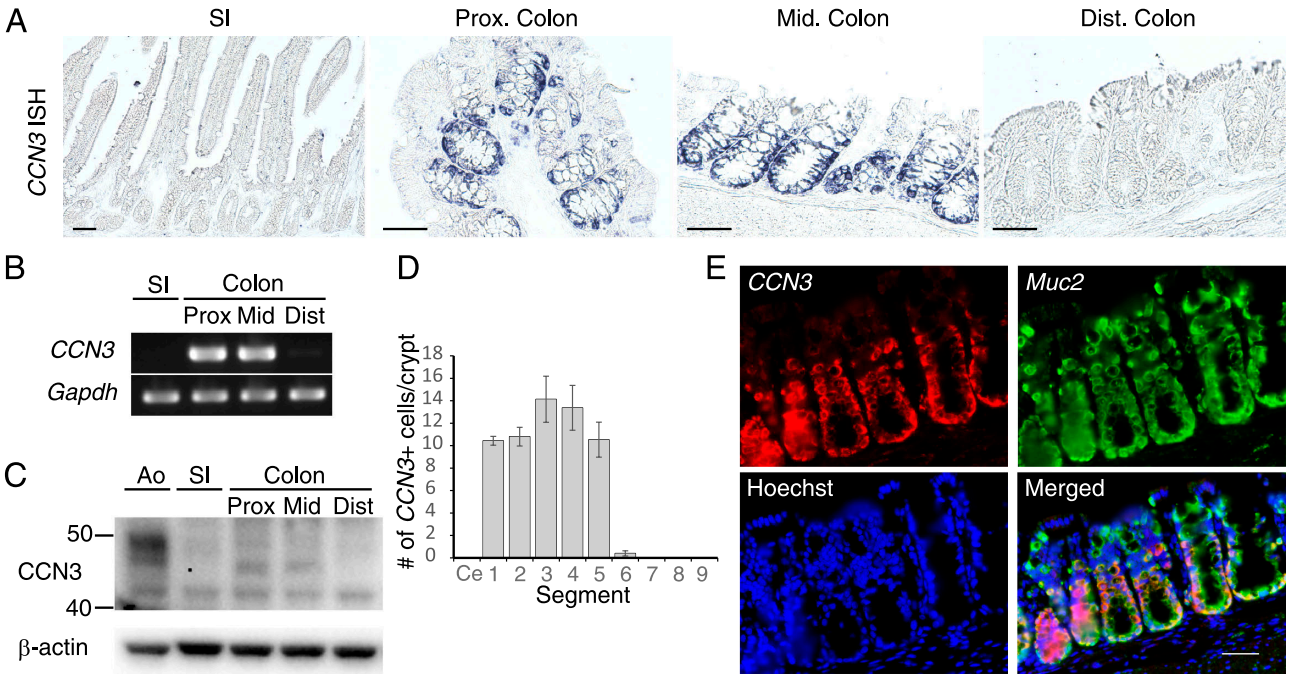

Fig. 2. *CCN3* is expressed in *Muc2*+ goblet cells in the proximal and middle colon. **A**: Expression of *CCN3* in the small intestine (SI), proximal (prox), middle (mid) and distal (dist) colon were assessed by *in situ* hybridization. Data are representative of three independent experiments. **B**: Total RNA was extracted from the crypts isolated from the small intestine, proximal, middle and distal colon. Semi-quantitative RT-PCR was performed for *CCN3* and *Gapdh*. Data are representative of three independent experiments. **C**: Whole lysates derived from the aorta (Ao) and each part of the intestine (SI, prox, mid, and dist colon) were immunoblotted for CCN3 and β-actin (loading control). Data are representative of three independent experiments. **D**: The number of *CCN3*+ cells per crypt was counted in full-length crypts on sections of the cecum (Ce) and 9 segments (segment 1–9) along the proximal-to-distal axis of the colon. Fifteen crypts originating from 3 individual mice were assessed in total for each intestinal segment and data are presented as mean ± s.e.m (n = 3). **E**: Co-expression of *CCN3* and *Muc2* in the middle colon assessed by double fluorescence ISH with a DIG-labeled *CCN3* probe and a FITC-labeled *Muc2* probe. Nuclear staining with Hoechst33342 and merged image are also shown. Data are representative of three independent experiments. Bars = 50 μm.

To gain more insight into the uneven distribution of *CCN3* expression along the longitudinal axis of the colon, we divided the entire length of colon into 9 segments and counted the number of *CCN3*+ cells per crypt on the ISH sections of each segment. The proximal 5 segments out of 9, designated as segments 1–5, contained more than 10 *CCN3*+ cells on average, with the segment 3 showing the highest value of 14.1 (±2.1) per crypt (Fig. 2D). No *CCN3*+ cells were detected in the segments 7–9 of the colon, small intestine and cecum (Fig. 2D), confirming the restricted pattern of *CCN3* expression.

Morphology of *CCN3*+ cells in the proximal and middle colon suggested that these cells might represent goblet cells (Fig. 2A). This appeared to be a reasonable assumption as we identified *CCN3* as a gene up-regulated by Notch signal inhibition, which induces intestinal cell differentiation towards secretory lineages. To test this hypothesis, we performed double fluorescence ISH with probes for *CCN3* and *Muc2*. *Muc2* probe labeled a number of cells located along the entire crypt axis in the middle colon, indicating that colon crypt cells are composed mostly of *Muc2*-producing goblet cells (Fig. 2E). *CCN3* mRNA was again found in cells located in lower crypts (Fig. 2E). As seen in the merged view, all *CCN3*+ cells showed positivity for *Muc2*, whereas *Muc2*+ cells extended more to upper crypts where *CCN3* mRNA was not detectable (Fig. 2E). Similar results were obtained when the proximal colon was analyzed (not shown). In the distal colon, despite the abundant presence of *Muc2*+ cells, *CCN3*+ cells were not detected (not shown). These observations suggested that *CCN3* was expressed in a particular subset of *Muc2*+ cells in lower crypts of the proximal and middle colon, whereas *CCN3*−/*Muc2*+ cells also constitute a subpopulation of goblet cells in these segments. In addition, the absence of *CCN3*+ cells in other intestinal segments (small intestine and distal colon) suggested that the Notch signaling is not the sole mechanism that regulates *CCN3* expression in the intestine.

Intestinal goblet cells, which are broadly visualized by AB staining, can be classified by HID staining that detects sulfated mucins [32, 33]. To analyze the distribution pattern of sulfomucin-producing goblet cells in the mouse intestine in detail, we performed HID staining on sections obtained from different segments of the intestine. In the small intestine, HID+ cells were sparsely scattered in both villi and crypts, and their staining showed complete overlap with the pattern of AB staining (Fig. 3A). AB+ cells were more abundant in the colon than in the small intestine (Fig. 3A). Notably, in the proximal and middle colon, HID staining

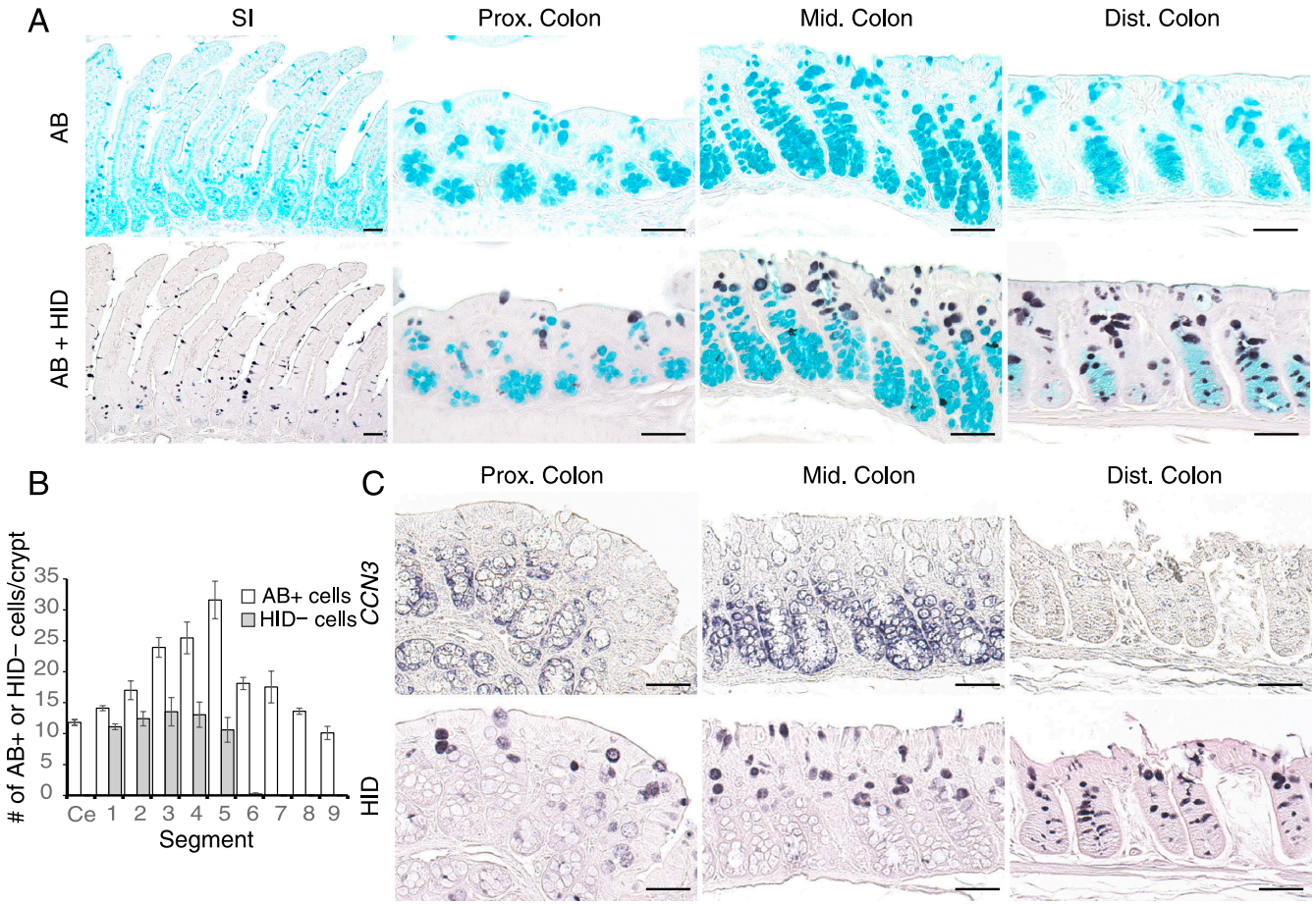

Fig. 3. *CCN3*+ cells coincide with AB+/HID− goblet cells. **A**: Serial sections of the small intestine, proximal, middle and distal colon were stained by AB and AB with HID (AB+HID). Data are representative of more than three independent experiments. **B**: The numbers of AB+ cells and HID− cells per crypt were counted as described in Fig. 2D. Fifteen crypts were assessed in total and data are presented as mean ± s.e.m (n = 3). **C**: ISH for *CCN3* (top) and HID staining (bottom) were performed on consecutive sections of the proximal, middle and distal colon. Data are representative of more than three independent experiments. Bars = 50 μm.

labeled only a subpopulation of AB+ cells in the upper crypts, clearly discriminating this population from HID−/AB+ cells predominantly localized in the lower crypt (Fig. 3A). In the distal colon, HID staining showed a different pattern. HID+ cells mostly coincided with the AB+ population and distributed along the entire crypt, although the size of granules stained by HID appeared to be smaller in the lower crypt than that in the upper part (Fig. 3A). These results proposed the presence of a unique subpopulation of intestinal goblet cells that are characterized as being AB+/HID− in the proximal and middle colon in mice. Furthermore, the unique distribution pattern of AB+/HID− cells suggested that this goblet cell subpopulation might correspond to *CCN3*+ cells. To test this hypothesis, we counted the number of HID+/HID− cells as well as AB+ cells per crypt on sections of 9 segments of the colon (Fig. 3B). The results showed that the number of AB+/HID− cells was almost the same as that of *CCN3*+ cells throughout the colon (Fig. 2D). We further assessed the relative distribution of HID+ cells and *CCN3*+ cells by conducting HID staining and *CCN3* ISH on consecutive sections, and found that the distribution patterns of *CCN3*+ cells and HID+ cells were mutually exclusive (Fig. 3C). These observations demonstrated that *CCN3* is expressed in a subpopulation of goblet cells that produce less or no sulfomucins and are localized only in the lower crypt of the proximal and middle colon.

Expression of CCN3 changes dynamically during the course of DSS-induced colitis

Depletion of goblet cells is one of the histological characteristics in many types of colitis. Although several studies showed the association between mucosal injuries and reduction of sulfomucins [21, 23], temporal behaviors of sulfomucin-producing and -nonproducing goblet cells during progression and recovery of colitis have remained unclear. Thus, we used the DSS-induced mouse colitis model [27] and monitored the time-course changes in the patterns of AB/HID staining and *CCN3* expression. In our experiments where 3% DSS was administered for 5 days,

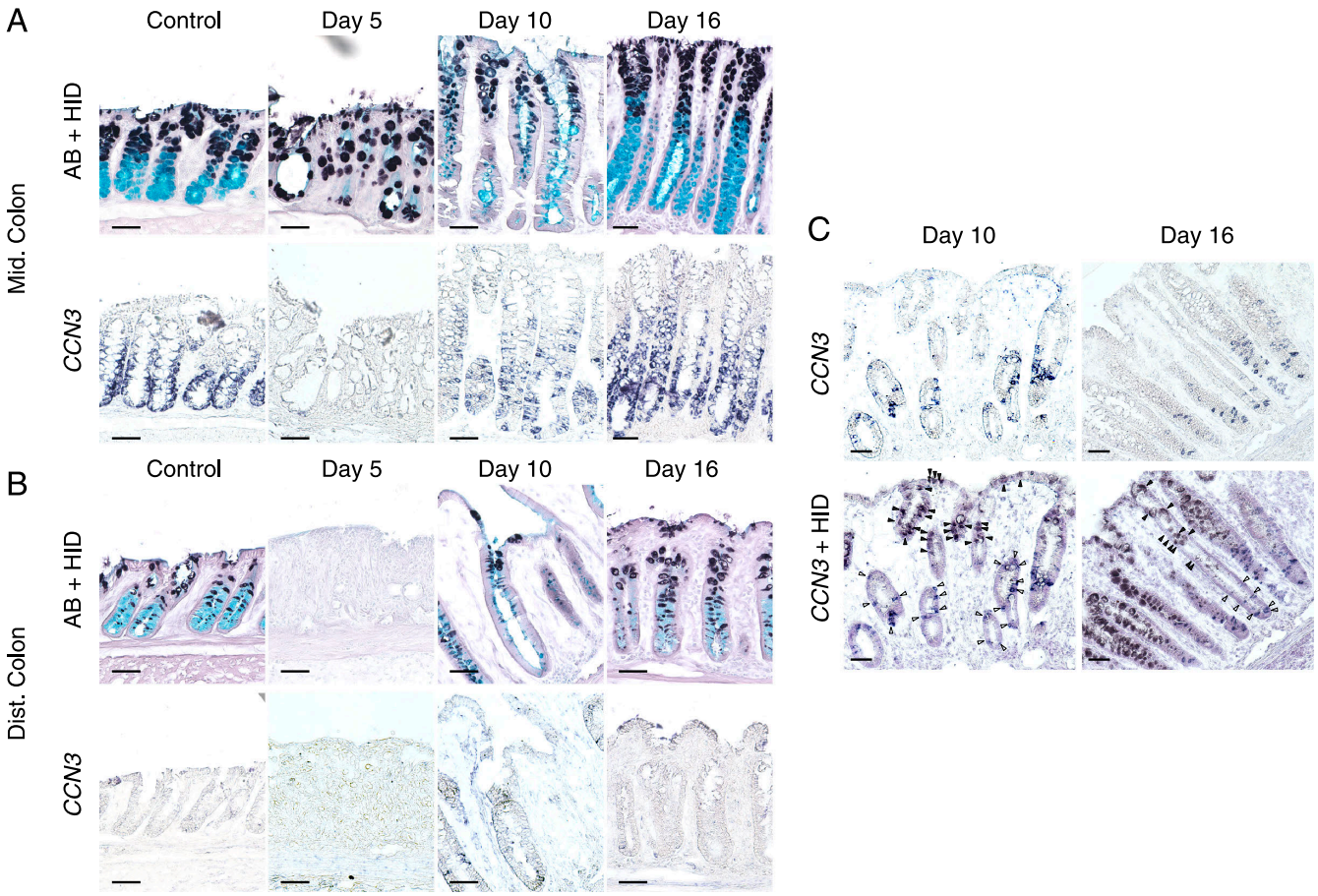

Fig. 4. Emergence of *CCN3*+, HID− goblet cells in the distal colon during recovery phase following colitis. Mice were treated with 3% DSS drinking water for 5 days. Tissues of the middle **A** and distal **B, C** colon were harvested on day 0 (pretreatment control), 5, 10, and 16 of DSS treatment, and subjected for AB + HID staining and ISH for *CCN3*. In **A** and **B**, consecutive sections were analyzed. In **C**, the section was first assayed for *CCN3* ISH (top, *CCN3*) and then stained by HID (bottom, *CCN3* + HID). Open and filled arrowheads point to *CCN3*+ cells and HID+ cells, respectively. Data are representative of three independent experiments. Bars = 50 μm.

mice developed acute colitis with clinical manifestations such as diarrhea and body weight loss, both of which typically peaked at around Day 10 of DSS administration [39]. They then showed mucosal repair and amelioration of clinical symptoms thereafter. Thus, we analyzed the colonic tissues on day 5, 10, and 16 of DSS administration. As previously reported [27], the mucosal damage in this model was prominent in the distal colon and was less severe in the middle colon. The proximal colon did not exhibit obvious mucosal damage or histological changes throughout the course of disease in our analysis (data not shown).

Analysis of the middle colon revealed destruction of crypt architecture on day 5 (Fig. 4A). The number of AB+ goblet cells was markedly reduced as compared with control tissues (Fig. 4A). Interestingly, although HID+ cells in the middle colon occurred only in upper crypts in controls (Fig. 4A, Fig. 3A), nearly all AB+ cells, from the bottom area to the top of the crypt, were HID+ at this time point. In addition, *CCN3* ISH on the adjacent section revealed that its expression disappeared on day 5 (Fig. 4A). Following this acute phase of colitis, tissue regeneration occurred through remarkable crypt elongation and expansion of AB+ goblet cell populations, as shown in the sections on day 10 and 16 (Fig. 4A). During this phase, localization of HID+ cells was again confined to the upper part of crypts, as seen in controls (Fig. 4A, Fig. 3A). In conjunction with this change, *CCN3*+ cells reappeared in the lower crypt, which mostly corresponded in position to AB+/HID− goblet cells (Fig. 4A). These observations suggested that, in the middle colon, the "goblet cell depletion" in the acute phase of colitis occurs with accompanying loss of HID−/*CCN3*+ goblet cells.

The distal colon displayed severe mucosal damage characterized by not only depletion of goblet cells but also disappearance of epithelial cells. In the acute phase (day 5), such severely injured areas contained few AB+ goblet cells (Fig. 4B). In later time points (day10 and 16), the distal colon mucosae showed different magnitudes of tissue repair even in the same individual. Areas that still displayed severe mucosal damage on day 10, which were recognized by distorted and irregularly distributed crypt structures, contained only few AB+ goblet cells (Fig. 4B, day 10). In

those injured areas, *CCN3*+ cells were almost absent (Fig. 4B). Meanwhile, even in the distal colon, some areas on day 16 showed fast tissue recovery from the damage, displaying almost normal morphology. In these areas, crypts were mostly composed of AB+/HID+ goblet cells, which were also shown to be *CCN3*−, as in control tissues of the distal colon (Fig. 4B). However, on sections of day 10 and 16 of the distal colon, we noticed an interesting phenomenon that occurred in areas undergoing active epithelial regeneration through prominent crypt elongation (Fig. 4C). *CCN3*+ cells, which were never observed in the normal distal colon, apparently emerged in the regenerating areas (Fig. 4C). These *CCN3*+ cells were localized in the lower part of elongated crypts, similar to *CCN3*+ cells observed in the middle colon during the recovery phase (Fig. 4A). To investigate whether these *CCN3*+ cells might be sulfomucin-producing cells or not, HID staining was subsequently performed on the same section following *CCN3* ISH. The result showed that, although the cells localized in the upper crypt were shown to be HID+, the *CCN3* cells that transiently and ectopically emerged in the distal colon were HID− (Fig. 4C), as were the *CCN3*+ cells present in the proximal and middle colon under both normal and colitic conditions.

IV. Discussion

We show here that *CCN3* is a gene induced by Notch signal inhibition in murine colon epithelial cells. In addition, we demonstrate that *CCN3* expression is confined to a subpopulation of goblet cells that are localized in the lower crypt of the proximal and middle colon. The present study is the first to demonstrate the unique distribution pattern of *CCN3* in a particular subset of colonic goblet cells in mice.

Intestinal goblet cells are generally characterized by their morphology and ability to produce a mucus component, Muc2 [2, 36]. However, previous studies demonstrated that they are not a uniform population of cells. For instance, a *cKit*+ population of colonic goblet cells was shown to be present at the crypt bottom and provide adjacent *Lgr5*-positive stem cells with niche signals [29]. Another report described that goblet cells in the surface epithelium of the colon, referred to as surface goblet cells, represent a distinct population from goblet cells along the crypts (crypt goblet cells) with regard to the rate of mucin biosynthesis and secretion [12]. We tested whether *CCN3*+ goblet cells described in our study might correspond to *cKit*+ cells by comparing the results of ISH for these genes. However, *CCN3* and *cKit* showed significant difference in distribution along the length of the intestine and depth of the crypt (not shown). The classification into surface and crypt goblet cells does not apply to *CCN3*+ or *CCN3*− cells either, as the two goblet cell types were seen in the distal colon [12], which lacks the *CCN3*+ population. Instead, we found that *CCN3*+ goblet cells correspond well to AB+/HID− goblet cells that are only seen in the proximal and middle colon in mice. This is consistent with a previous study in which sulfomucin-nonproducing, HID− goblet cells were shown to be abundantly detectable in the lower crypts of the rat proximal colon [32]. Another study also showed that this unique population of goblet cells, existing in the lower crypts of the proximal colon in rats, has morphologically distinct features when assessed by transmission electron microscopy [1]. We thus suggest that *CCN3* would become a molecular marker that identifies a subset of colonic goblet cells previously recognized by their unique localization, lack of ability to produce sulfated mucins, or ultrastructural features. Further study to characterize the function of this goblet cell population and its relationship with the molecular function of *CCN3* would be important to understand a variety of goblet cell functions and their region-specific regulation along the proximal-to-distal or crypt axis in the colon.

We also demonstrate that distribution of *CCN3*+ goblet cells dynamically changes during the progression and repair phases of DSS-induced acute colitis. The most interesting observation is that *CCN3*+ cells, which are not detectable in the normal distal colon, appear in the distal colon during the regeneration process of injured epithelia. Double fluorescence ISH with probes for *CCN3* and *Muc2* showed that the ectopically emerging *CCN3*+ cells are all positive for *Muc2* (not shown), indicating that they constitute a subpopulation of *Muc2*+ colonic goblet cells. These colitis-induced *CCN3*+ goblet cells in the distal colon are HID−, further suggesting the association of *CCN3* expression with the lack of ability to produce sulfomucins. Moreover, the *CCN3*+/HID− goblet cells are spatially confined to the lower crypt but absent in the upper crypt and surface epithelium when they are detected in the distal colon following colitis (Fig. 4C). All these observations suggest that the *CCN3*+ cells that ectopically emerge in the distal colon share many common features with *CCN3*+ cells in the proximal and middle colon in normal mice. In addition, the complete absence of *CCN3*+ cells in the fully repaired distal colon (Fig. 4B) suggests that the changes of the distal colonic epithelium during regeneration, which show some phenotypic similarity with the proximal and middle colon, are not mediated by irreversible cellular changes but by reversible and transient alteration associated with repair process.

It remains unclear as to what is the regulatory mechanism of *CCN3* expression in the distal colon. In this study, we have identified *CCN3* as a gene negatively regulated by Notch signaling in the colonic epithelium. Based on the findings that the Notch signaling contributes not only to cellular differentiation but also to proliferation of immature cells of the intestine [7, 26], our data showing dynamic changes in *CCN3* expression in the middle colon during tissue regeneration, i.e. the significant decrease in the acute phase of colitis and increase in the regenerative phase, may represent the hyperactive and hypoactive states of Notch signaling during tissue repair in this colonic

region (Fig. 4A). However, considering that the Notch signaling is functional throughout the entire length of the colon [20], it is suggested that, under normal circumstances, *CCN3* expression in the distal colon is controlled not only by Notch signaling but also through some other unknown mechanisms. Moreover, the transient and ectopic emergence of *CCN3*+ cells in the distal colon in the DSS colitis model further proposes an idea that the epithelial repair process following injury in this particular region of the colon may not be a mere acceleration of immature cell proliferation but be additionally mediated by such unknown mechanisms to produce *CCN3*+/HID− goblet cell populations.

We believe that further studies on what is the function of *CCN3*+ goblet cells and how they ectopically emerge in the distal colon during the recovery phase of colitis are beneficial to understand the mechanism of epithelial regeneration following injury.

V. Conflict of Interest

The authors declare that they have no conflict of interest.

VI. Acknowledgments

This study was supported by MEXT KAKENHI (Grant number 26112705), JSPS KAKENHI (24390186 and 26221307), the Regenerative Medicine Realization Base Network Program from the Japan Science and Technology Agency.

VII. References

1. Altmann, G. G. (1983) Morphological observations on mucus-secreting nongoblet cells in the deep crypts of the rat ascending colon. *Am. J. Anat.* 167; 95–117.
2. Birchenough, G. M., Johansson, M. E., Gustafsson, J. K., Bergstrom, J. H. and Hansson, G. C. (2015) New developments in goblet cell mucus secretion and function. *Mucosal Immunol.* 8; 712–719.
3. Brenna, O., Furnes, M. W., Munkvold, B., Kidd, M., Sandvik, A. K. and Gustafsson, B. I. (2016) Cellular localization of guanylin and uroguanylin mRNAs in human and rat duodenal and colonic mucosa. *Cell Tissue Res.* 365; 331–341.
4. Chevalier, G., Yeger, H., Martinerie, C., Laurent, M., Alami, J., Schofield, P. N. and Perbal, B. (1998) novH: differential expression in developing kidney and Wilm's tumors. *Am. J. Pathol.* 152; 1563–1575.
5. Droy-Dupre, L., Vallee, M., Bossard, C., Laboisse, C. L. and Jarry, A. (2012) A multiparametric approach to monitor the effects of gamma-secretase inhibition along the whole intestinal tract. *Dis. Model. Mech.* 5; 107–114.
6. Forman, R. A., deSchoolmeester, M. L., Hurst, R. J., Wright, S. H., Pemberton, A. D. and Else, K. J. (2012) The goblet cell is the cellular source of the anti-microbial angiogenin 4 in the large intestine post Trichuris muris infection. *PLoS One* 7; e42248.
7. Fre, S., Huyghe, M., Mourikis, P., Robine, S., Louvard, D. and Artavanis-Tsakonas, S. (2005) Notch signals control the fate of immature progenitor cells in the intestine. *Nature* 435; 964–968.
8. Fukuda, M., Mizutani, T., Mochizuki, W., Matsumoto, T., Nozaki, K., Sakamaki, Y., Ichinose, S., Okada, Y., Tanaka, T., Watanabe, M. and Nakamura, T. (2014) Small intestinal stem cell identity is maintained with functional Paneth cells in heterotopically grafted epithelium onto the colon. *Genes Dev.* 28; 1752–1757.
9. Gupta, R., Hong, D., Iborra, F., Sarno, S. and Enver, T. (2007) NOV (CCN3) functions as a regulator of human hematopoietic stem or progenitor cells. *Science* 316; 590–593.
10. Jenny, M., Uhl, C., Roche, C., Duluc, I., Guillermin, V., Guillemot, F., Jensen, J., Kedinger, M. and Gradwohl, G. (2002) Neurogenin3 is differentially required for endocrine cell fate specification in the intestinal and gastric epithelium. *EMBO J.* 21; 6338–6347.
11. Jensen, J., Pedersen, E. E., Galante, P., Hald, J., Heller, R. S., Ishibashi, M., Kageyama, R., Guillemot, F., Serup, P. and Madsen, O. D. (2000) Control of endodermal endocrine development by Hes-1. *Nat. Genet.* 24; 36–44.
12. Johansson, M. E. (2012) Fast renewal of the distal colonic mucus layers by the surface goblet cells as measured by in vivo labeling of mucin glycoproteins. *PLoS One* 7; e41009.
13. Jun, J. I. and Lau, L. F. (2011) Taking aim at the extracellular matrix: CCN proteins as emerging therapeutic targets. *Nat. Rev. Drug Discov.* 10; 945–963.
14. Katsube, K., Ichikawa, S., Katsuki, Y., Kihara, T., Terai, M., Lau, L. F., Tamamura, Y., Takeda, S., Umezawa, A., Sakamoto, K. and Yamaguchi, A. (2009) CCN3 and bone marrow cells. *J. Cell Commun. Signal.* 3; 135–145.
15. Komiya, T., Tanigawa, Y. and Hirohashi, S. (1999) Cloning and identification of the gene gob-5, which is expressed in intestinal goblet cells in mice. *Biochem. Biophys. Res. Commun.* 255; 347–351.
16. Kular, L., Pakradouni, J., Kitabgi, P., Laurent, M. and Martinerie, C. (2011) The CCN family: a new class of inflammation modulators? *Biochimie* 93; 377–388.
17. Lin, C. G., Leu, S. J., Chen, N., Tebeau, C. M., Lin, S. X., Yeung, C. Y. and Lau, L. F. (2003) CCN3 (NOV) is a novel angiogenic regulator of the CCN protein family. *J. Biol. Chem.* 278; 24200–24208.
18. Lin, C. G., Chen, C. C., Leu, S. J., Grzeszkiewicz, T. M. and Lau, L. F. (2005) Integrin-dependent functions of the angiogenic inducer NOV (CCN3): implication in wound healing. *J. Biol. Chem.* 280; 8229–8237.
19. Lin, Z., Natesan, V., Shi, H., Hamik, A., Kawanami, D., Hao, C., Mahabaleshwar, G. H., Wang, W., Jin, Z. G., Atkins, G. B., Firth, S. M., Rittie, L., Perbal, B. and Jain, M. K. (2010) A novel role of CCN3 in regulating endothelial inflammation. *J. Cell Commun. Signal.* 4; 141–153.
20. Lo, Y. H., Chung, E., Li, Z., Wan, Y. W., Mahe, M. M., Chen, M. S., Noah, T. K., Bell, K. N., Yalamanchili, H. K., Klisch, T. J., Liu, Z., Park, J. S. and Shroyer, N. F. (2017) Transcriptional Regulation by ATOH1 and its Target SPDEF in the Intestine. *Cell. Mol. Gastroenterol. Hepatol.* 3; 51–71.
21. Makkink, M. K., Schwerbrock, N. M., Mahler, M., Boshuizen, J. A., Renes, I. B., Cornberg, M., Hedrich, H. J., Einerhand, A. W., Buller, H. A., Wagner, S., Enss, M. L. and Dekker, J. (2002) Fate of goblet cells in experimental colitis. *Dig. Dis. Sci.* 47; 2286–2297.
22. Milano, J., McKay, J., Dagenais, C., Foster-Brown, L., Pognan, F., Gadient, R., Jacobs, R. T., Zacco, A., Greenberg, B. and Ciaccio, P. J. (2004) Modulation of notch processing by gamma-secretase inhibitors causes intestinal goblet cell metaplasia and induction of genes known to specify gut secretory lineage differentiation. *Toxicol. Sci.* 82; 341–358.

23. Nakano, S., Ohara, S., Kubota, T., Saigenji, K. and Hotta, K. (1999) Compensatory response of colon tissue to dextran sulfate sodium-induced colitis. *J. Gastroenterol.* 34; 207–214.
24. Noah, T. K., Kazanjian, A., Whitsett, J. and Shroyer, N. F. (2010) SAM pointed domain ETS factor (SPDEF) regulates terminal differentiation and maturation of intestinal goblet cells. *Exp. Cell Res.* 316; 452–465.
25. Noah, T. K. and Shroyer, N. F. (2013) Notch in the intestine: regulation of homeostasis and pathogenesis. *Annu. Rev. Physiol.* 75; 263–288.
26. Okamoto, R., Tsuchiya, K., Nemoto, Y., Akiyama, J., Nakamura, T., Kanai, T. and Watanabe, M. (2009) Requirement of Notch activation during regeneration of the intestinal epithelia. *Am. J. Physiol. Gastrointest. Liver Physiol.* 296; G23–35.
27. Okayasu, I., Hatakeyama, S., Yamada, M., Ohkusa, T., Inagaki, Y. and Nakaya, R. (1990) A novel method in the induction of reliable experimental acute and chronic ulcerative colitis in mice. *Gastroenterology* 98; 694–702.
28. Rindi, G., Buffa, R., Sessa, F., Tortora, O. and Solcia, E. (1986) Chromogranin A, B and C immunoreactivities of mammalian endocrine cells. Distribution, distinction from costored hormones/prohormones and relationship with the argyrophil component of secretory granules. *Histochemistry* 85; 19–28.
29. Rothenberg, M. E., Nusse, Y., Kalisky, T., Lee, J. J., Dalerba, P., Scheeren, F., Lobo, N., Kulkarni, S., Sim, S., Qian, D., Beachy, P. A., Pasricha, P. J., Quake, S. R. and Clarke, M. F. (2012) Identification of a cKit(+) colonic crypt base secretory cell that supports Lgr5(+) stem cells in mice. *Gastroenterology* 142; 1195–1205 e1196.
30. Sakamoto, K., Yamaguchi, S., Ando, R., Miyawaki, A., Kabasawa, Y., Takagi, M., Li, C. L., Perbal, B. and Katsube, K. (2002) The nephroblastoma overexpressed gene (NOV/ccn3) protein associates with Notch1 extracellular domain and inhibits myoblast differentiation via Notch signaling pathway. *J. Biol. Chem.* 277; 29399–29405.
31. Searfoss, G. H., Jordan, W. H., Calligaro, D. O., Galbreath, E. J., Schirtzinger, L. M., Berridge, B. R., Gao, H., Higgins, M. A., May, P. C. and Ryan, T. P. (2003) Adipsin, a biomarker of gastrointestinal toxicity mediated by a functional gamma-secretase inhibitor. *J. Biol. Chem.* 278; 46107–46116.
32. Shamsuddin, A. K. and Trump, B. F. (1981) Colon epithelium. I. Light microscopic, histochemical, and ultrastructural features of normal colon epithelium of male Fischer 344 rats. *J. Natl. Cancer Inst.* 66; 375–388.
33. Spicer, S. S. (1965) Diamine methods for differentialing mucosubstances histochemically. *J. Histochem. Cytochem.* 13; 211–234.
34. Su, B. Y., Cai, W. Q., Zhang, C. G., Martinez, V., Lombet, A. and Perbal, B. (2001) The expression of ccn3 (nov) RNA and protein in the rat central nervous system is developmentally regulated. *Mol. Pathol.* 54; 184–191.
35. van Es, J. H., van Gijn, M. E., Riccio, O., van den Born, M., Vooijs, M., Begthel, H., Cozijnsen, M., Robine, S., Winton, D. J., Radtke, F. and Clevers, H. (2005) Notch/gamma-secretase inhibition turns proliferative cells in intestinal crypts and adenomas into goblet cells. *Nature* 435; 959–963.
36. van Klinken, B. J., Einerhand, A. W., Duits, L. A., Makkink, M. K., Tytgat, K. M., Renes, I. B., Verburg, M., Buller, H. A. and Dekker, J. (1999) Gastrointestinal expression and partial cDNA cloning of murine Muc2. *Am. J. Physiol.* 276; G115–124.
37. Watakabe, A., Ichinohe, N., Ohsawa, S., Hashikawa, T., Komatsu, Y., Rockland, K. S. and Yamamori, T. (2007) Comparative analysis of layer-specific genes in Mammalian neocortex. *Cereb. Cortex* 17; 1918–1933.
38. Yang, Q., Bermingham, N. A., Finegold, M. J. and Zoghbi, H. Y. (2001) Requirement of Math1 for secretory cell lineage commitment in the mouse intestine. *Science* 294; 2155–2158.
39. Yui, S., Nakamura, T., Sato, T., Nemoto, Y., Mizutani, T., Zheng, X., Ichinose, S., Nagaishi, T., Okamoto, R., Tsuchiya, K., Clevers, H. and Watanabe, M. (2012) Functional engraftment of colon epithelium expanded in vitro from a single adult Lgr5(+) stem cell. *Nat. Med.* 18; 618–623.
40. Zhang, C., van der Voort, D., Shi, H., Zhang, R., Qing, Y., Hiraoka, S., Takemoto, M., Yokote, K., Moxon, J. V., Norman, P., Rittie, L., Kuivaniemi, H., Atkins, G. B., Gerson, S. L., Shi, G. P., Golledge, J., Dong, N., Perbal, B., Prosdocimo, D. A. and Lin, Z. (2016) Matricellular protein CCN3 mitigates abdominal aortic aneurysm. *J. Clin. Invest.* 126; 1282–1299.